

Characterization of Randomly Branched Polymers Formed by End-Linking Linear Polystyrene Using Controlled Free Radical Polymerization

Pascal Ourdouillie and Philippe Chaumont

Laboratoire des Matériaux Polymères et des Biomatériaux, UMR CNRS No. 5627, Université Claude Bernard, Lyon 1, 43 Bd 11 Novembre 1918, F-69622 Villeurbanne Cedex, France

Françoise Mechin and Michel Dumon

Laboratoire des Matériaux Macromoléculaires, UMR CNRS No. 5627, INSA de Lyon, 20 rue Albert Einstein, F-69621 Villeurbanne Cedex, France

Dominique Durand and Taco Nicolai*

Polymères, Colloïdes, Interfaces, UMR CNRS 6120, Université du Maine, 72085 Le Mans Cedex 9, France

Received January 22, 2001; Revised Manuscript Received March 5, 2001

ABSTRACT: Randomly branched polystyrene (PS) was synthesized by end-linking monodisperse linear PS chains with divinylbenzene using controlled free radical polymerization. Samples obtained at different reaction extents were characterized using size exclusion chromatography and static and dynamic light scattering. The results are compared with those obtained on randomly branched poly(methyl methacrylate) (PMMA). The overall structure of branched PS was found to be the same as that of branched PMMA despite the very different local structure. The results strongly support the idea that the formation of polymeric gels is a universal process that may be described by the percolation model.

Introduction

Polymeric gels may be formed by copolymerization of difunctional monomers in the presence of multifunctional monomers that act as cross-link agents. Alternatively, they may be formed by cross-linking precursor polymers. In both cases randomly branched polymers are formed which grow in size until a system spanning gel is formed. It has been suggested that the percolation model describes the growth process close to the gel point when the branched polymers are strongly interpenetrated.¹ Numerical simulations of the percolation model showed that percolating clusters have a self-similar structure and a power law mass distribution.² The molar mass distribution ($N(M)$) of percolating clusters is

$$N(M) \propto M^{-\tau} f(M/M^*) \quad M \gg M_0 \quad (1)$$

where M_0 is the molar mass of the smallest particle in the distribution, $\tau = 2.2^3$ is the polydispersity exponent, and $f(M/M^*)$ is a cutoff function at a characteristic molar mass M^* . The pair correlation function of percolating clusters is

$$g(r) \propto r^{d_f-3} f(r/R_g) \quad r \gg r_0 \quad (2)$$

with $d_f = 2.53$ the fractal dimension,⁴ r_0 the size of the elementary units, and $f(r/R_g)$ another cutoff function. It follows from eq 2 that the molar mass scales with the radius of gyration: $M \propto R_g^{d_f}$.

The percolation model describes random site or bond occupation on a lattice. Clearly, such a model can only claim to describe the structure of real systems at length scales much larger than that of the precursors. In addition, the model does not consider mobility and flexibility of the clusters. However, numerical simula-

tions of a system in which the clusters are allowed to diffuse and stick when they touch each other (diffusion-limited cluster aggregation) show that the structure and size distribution of the clusters approaches that of percolating clusters once the clusters occupy the entire volume and begin to overlap.⁵

The gel formation has also been described using mean-field theory.⁶ However, this theory neglects excluded-volume interaction and cyclization. Mean-field theory predicts that the density of the clusters increases linearly with their size $M \propto R_g^4$ and has a power law mass distribution with $\tau = 2.5$. Notice that mean-field theory does not predict the formation of clusters with a self-similar structure, but clusters that are homogeneous ($d_f = 3$) at large length scales and have a local structure that densifies with increasing size. The assumptions of mean-field theory may be reasonable for small clusters with low density but are bound to fail for large clusters.

Experimentally, the mass distribution of branched polymers may be investigated using size exclusion chromatography (SEC). Such investigations have been done for various systems^{7–10} and seem to show that the mass distribution of branched polymers close to the gel point is compatible with that of percolating clusters. However, there are serious experimental limitations to the use of SEC to study the large branched polymers for which eq 1 may be applied; see ref 11 for a detailed discussion of this issue. A different method to obtain the mass distribution is dynamic light scattering (DLS). This method was used for one system¹² and showed that the mass distribution of randomly branched poly(methyl methacrylate) (PMMA) close to the gel point is compatible with that of percolating clusters.

The structure of branched polymers may be studied using light scattering.¹³ From the scattering wave vector

(q) dependence of the scattered light one obtains the static structure factor ($S(q)$). In highly diluted solutions interactions between the branched polymers may be neglected, and $S(q)$ is equal to the Fourier transform of $g(r)$. With light scattering the structure may be studied at much larger length scales than the distance between cross-links and is therefore an excellent method to check the validity of the percolation model. However, before the comparison can be made, one needs to consider the influence of dilution. Before diluting, excluded-volume interactions between segments of a branched polymer are partially screened by the presence of other interpenetrating polymers. After diluting, excluded-volume interactions swell the branched polymers. It has been argued that the fractal dimension of percolating clusters swollen in good solvents is 2.0.¹⁴ One also needs to consider the polydispersity. With light scattering the z -average structure factor ($S_z(q)$), the weight-average molar mass (M_w), and the z -average radius of gyration (R_{gz}) are measured. The experimentally observed fractal dimension, d_f^* , using either $S_z(q) \propto q^{-d_f^*}$ or $M_w \propto R_{gz}^{-d_f^*}$ is related to the fractal dimension of the branched polymers as $d_f^* = d_f(3-\tau)$ if $\tau > 2$.² It follows that the measured fractal dimension of swollen polydisperse percolating clusters is 1.6.

Recently, a detailed characterization was reported of the gel formation during free radical copolymerization of methyl methacrylate (MMA) and ethyl glycol dimethyl methacrylate (EGDMA).^{10,15,16} In this system initially rather polydisperse linear PMMA chains are formed with tetrafunctional EGDMA segments incorporated at random positions. With increasing reaction extent the concentration of PMMA increases, which in turn increases the probability of branching. When the PMMA chains begin to overlap, branching becomes important and leads to gel formation. The results obtained for this system were compatible with the hypothesis that randomly branched polymers formed close to the gel point have the size distribution and large-scale structure of percolating clusters. The same conclusion was reached earlier for randomly branched polymers formed by end-linking monodisperse linear poly(dimethylsiloxane) (PDMS) chains using a tetrafunctional cross-linking agent.¹⁷

In the system we are considering here the gel is synthesized in two separate steps. In the first step monodisperse linear polystyrene (PS) is formed by nitroxide-controlled free radical polymerization. In the second step divinylbenzene (DVB) is added, which cross-links the PS chain ends. Details of the synthesis method and the swelling properties of the fully reacted gels are reported elsewhere.¹⁸

The local structure of the branched polymers and gels of cross-linked PS is very different from that of cross-linked PMMA even though in both cases randomly branched polymers are formed by free radical copolymerization of bifunctional and polyfunctional monomers. For cross-linked PMMA the functionality of the branch points is everywhere the same, but the distance between two branch points varies widely. On the other hand, for cross-linked PS the distance between two branch points is everywhere the same, but the functionality of the branch points varies and increases with increasing reaction extent.

Despite the very different local structure, the large-length-scale structure should be the same for branched PMMA and branched PS if the percolating model gives

the correct description of the gel formation. The object of the present article is to compare the large-scale structure of branched PS with that of branched PMMA. In this way we can establish whether the gel formation is universal for polymeric systems with very different local structure.

Experimental Section

Materials. Linear precursor polystyrene was prepared by controlled free radical polymerization of styrene in the bulk using a method described elsewhere.¹⁸ Branched PS samples were obtained by heating sealed tubes containing solutions of precursor PS and DVB in xylene. Precursor PS acts as a macroinitiator for the cross-linking polymerization of DVB. Samples with different reaction extents were prepared by heating for different lengths of time followed by rapid cooling to room temperature which stops the reaction.

The samples were highly diluted in xylene and filtered through Anatop filters with 0.22 μm pore size to remove spurious scatterers. Samples close to the gel point were not filtered because they contained very large branched PS which would be removed by filtration. Fortunately, the scattering intensity of large polymers is strong so that the effect of spurious scatterers is very small.

Methods. Light scattering measurements were made using an ALV-5000 multibit, multitau full digital correlator in combination with a Malvern goniometer and a Spectra-Physics laser emitting vertically polarized light at $\lambda = 532$ nm. The temperature is controlled by a thermostat bath set at 20 °C. The relative excess scattering intensity (I_r) was calculated as the total scattered light intensity minus the solvent scattering divided by the scattering intensity of toluene.

In general, I_r can be written as¹⁹

$$I_r = KCM_w S(q) \quad (3)$$

where $S(q)$ is the structure factor which expresses the scattering wave vector dependence of the scattering intensity ($q = 4\pi n_s \sin(\theta/2)/\lambda$, with θ the angle of observation and n_s the refractive index of the solution) and K is a contrast factor:

$$K = \frac{4\pi^2 n_s^2}{\lambda^4 N_a} \left(\frac{\partial n}{\partial C} \right)^2 \left(\frac{n_{\text{tol}}}{n_s} \right)^2 \frac{1}{R_{\text{tol}}} \quad (4)$$

Here N_a is Avogadro's number, $\partial n/\partial C$ is the refractive index increment, and R_{tol} is the Rayleigh ratio of toluene at 20 °C ($2.79 \times 10^{-5} \text{ cm}^{-1}$ at $\lambda = 532 \text{ nm}$ ²⁰). $(n_{\text{tol}}/n_s)^2$ corrects for the difference in scattering volume of the solution and the toluene standard with refractive index n_{tol} . In the calculation of K we have used $\partial n/\partial C = 0.11 \text{ mL/g}$.²¹ For very dilute solutions interactions may be neglected, and $S(q)$ depends only on the structure of the solute. From the initial q dependence of $S(q)$ we may calculate the z -average radius of gyration (R_{gz}) using the so-called Zimm approximation:

$$\frac{KC}{I_r} = \frac{1}{M_w} \left(1 + \frac{1}{3} (qR_{gz})^2 \right) \quad qR_{gz} < 1 \quad (5)$$

With dynamic light scattering (DLS) the intensity autocorrelation function is measured which is related to the field autocorrelation function ($g_1(t)$) via the so-called Siegert relation.²² All correlation functions reported in the present study were characterized by a single monomodal relaxation time distribution:

$$g_1(t) = \int A(\log \tau) \exp(-t/\tau) d \log \tau \quad (6)$$

The data were fitted using a generalized exponential distribution:²³

$$A(\log \tau) = k\tau^p \exp[-(\tau/\tau^*)^s] \quad (7)$$

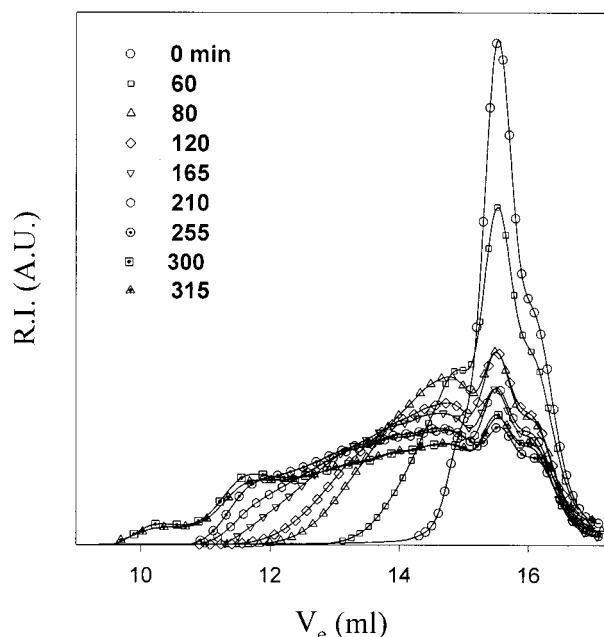


Figure 1. Chromatograms of branched PS formed at different heating times indicated in the figure.

This versatile function contains two parameters (p , s) to describe the shape of a wide range of single peaked distributions such as the Schultz–Zimm and the Pearson distribution. τ^* is the characteristic relaxation time, and k is a normalization constant. The apparent diffusion coefficient D_a was determined from the average relaxation rate $\langle \Gamma \rangle = \langle \tau^{-1} \rangle$: $D_a = \langle \Gamma \rangle / q^2$.

Size exclusion chromatography measurements were done using two PL-Gel columns (Polymer Laboratories, type “Mixed” and “Mixed B”) in series. The eluant was THF and the flow rate 1 cm³/min. The concentration was monitored by a differential refractometer (R410 from Millipore-Waters).

Results and Discussion

A series of branched PS samples were prepared using precursor PS with $M_w = 10^4$ g/mol and DVB with molar ratio [DVB]/[PS] = 10. Solutions containing 250 g/L precursor PS in xylene were heated for set periods of time at 120 °C. After about 330 min the solution does not flow any longer if the sample is tilted, and a self-supporting gel is formed. It is necessary to homogenize the samples regularly; otherwise, the gel is formed first at the bottom of the tube and then extends with heating time until the whole system has gelled. A similar inhomogeneous gelation was observed for the free radical copolymerization of MMA and EGDMA.

The samples at different heating times (t_h) before the gel point were analyzed using SEC and static and dynamic light scattering. Figure 1 shows the size distribution of branched polymers formed at different reaction times. Before heating, the system contains a relatively narrow distribution of linear PS ($M_w/M_n = 1.2$). With increasing heating time more and more PS chains are end-linked by DVB and the distribution of branched PS broadens. A gel is formed when the largest branched polymers span the whole volume. An important observation is that the maximum of the distribution does not shift to smaller elution volume (V_e) but remains situated at V_e of the linear precursors. This is generally observed for branched polymers formed by cross-linking overlapping polymers.^{7–10}

This feature can be explained by assuming that, in first approximation, the branched polymers have a

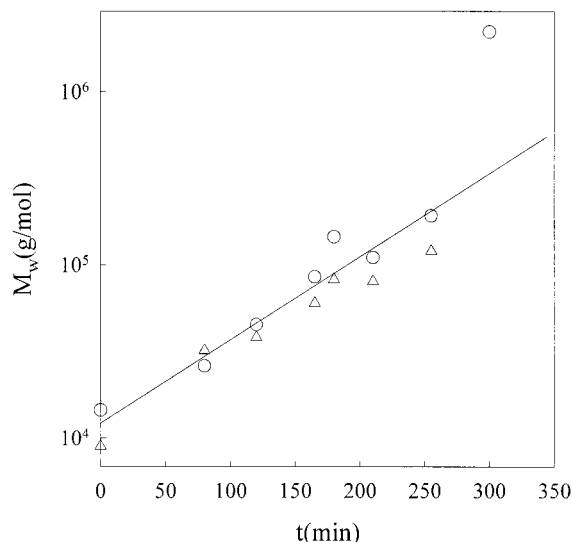


Figure 2. Semilogarithmic representation of the evolution with heating time of M_w of branched PS. Data obtained from light scattering (circles) are compared with data obtained from SEC with using calibration with linear PS standards (triangles). The straight line shows that the initial increase is exponential.

power law mass distribution (see eq 1). The refractive index signal (RI) is proportional to the polymer concentration ($C = MN(M)$) and has the following molar mass dependence: $RI \propto M^{-\tau+1} f(M/M^*)$. If we assume further that $V_{el} \propto \ln(M)$, it follows that $RI \propto V_e^{-\tau+2}$ so that the maximum of RI is situated at the upper limit of the mass distribution for $\tau < 2$ and at the lower limit, i.e., at the precursors, if $\tau > 2$. Of course, the assumption that $V_{el} \propto \ln(M)$ is only approximate because the precursors are linear and the larger polymers are branched. In addition, it is obvious from Figure 1 that the mass distribution does not follow a smooth power law. The chromatographs contain oscillations that were observed earlier for several other cross-linked polymers.^{7,8,10} It is not clear whether the oscillations are an artifact of the separation technique or a true feature of the mass distribution. Nevertheless, even if the assumptions are only approximately right, the SEC results indicate that $\tau > 2$ as is the case for percolating clusters.

In principle, a value of τ may be extracted from the chromatographs as was done for cross-linked PMMA which gave $\tau \approx 2.3$.¹⁰ However, as was discussed in detail in ref 12, the correct exponent is only observed for very large clusters, i.e., close to and beyond the resolution limit of the SEC columns. In addition, the oscillations on the chromatographs preclude an accurate determination of τ . Therefore, we made no attempt to extract a value for τ from the data shown in Figure 1.

Values of M_w were determined using light scattering (see Experimental Section) and are plotted in Figure 2 as a function of heating time. For comparison, we also show the values obtained from SEC using the calibration curve for linear PS. These values are systematically lower for the larger polymers because branched PS is denser than linear PS. M_w increases initially approximately exponentially but diverges close to the gel point. Such behavior is expected for reaction-limited growth in the early stages of the reaction followed by percolation once the branched polymers begin the overlap.

At short times the branched polymers are too small to show a significant q dependence of I_r . The q depen-

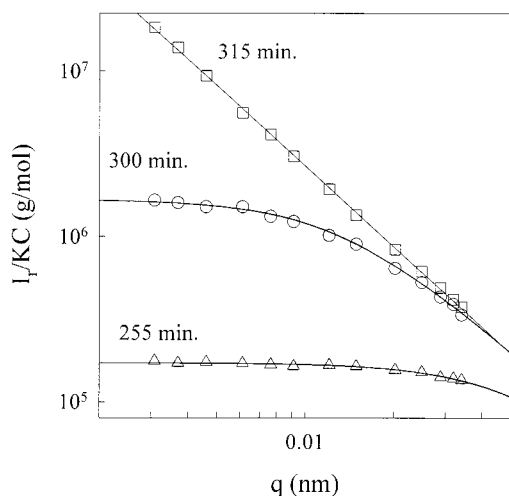


Figure 3. Double-logarithmic representation of the q dependence of I_r/KC at different heating times indicated in the figure. The straight line represents a linear least-squares fit and has slope -1.6 . The curved lines are guides to the eye.

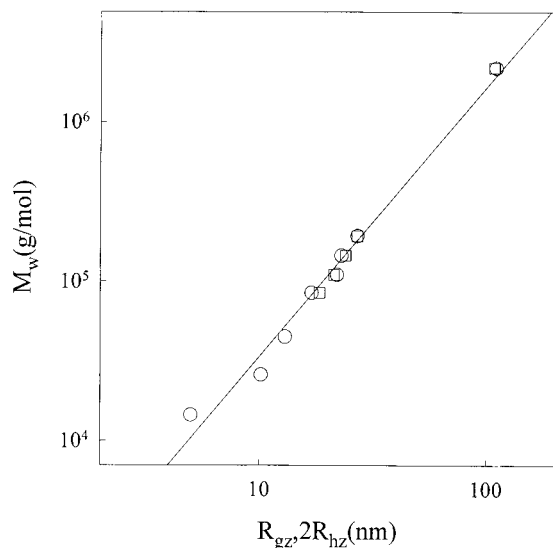


Figure 4. Double-logarithmic representation of M_w vs R_{gz} (squares) and $2R_{hz}$ (circles). The straight line represents a linear least-squares fit and has slope 1.6 .

dence of I_r of the samples formed at longer heating times is shown in Figure 3. From the initial curvature we calculated R_{gz} , which is plotted as a function of M_w in Figure 4. At $t_h = 315$ min, i.e., close to the gel time, the sample contains very large branched polymers ($R_{gz} > 1 \mu\text{m}$), and I_r has a power law q dependence over the whole accessible range. As was discussed in the Introduction, the power law q dependence implies that the particles have a self-similar structure. A linear least-squares analysis of the data gives $d_f^* = 1.6$, which is close to the value observed for cross-linked PMMA¹⁶ and for cross-linked PDMS.¹⁷

The static structure factors obtained at different times superimpose if we plot them as a function of qR_{gz} (see Figure 5). This means that the branched polymers have the same self-similar structure and size distribution at different reaction times. Results obtained with precursor PS chains with $M_w = 1.7 \times 10^4$ g/mol give similar results and are shown for comparison in Figure 5. The solid line through the data represents the structure factor of cross-linked PMMA¹⁶ and demonstrates that within the experimental error end-linked PS and cross-linked

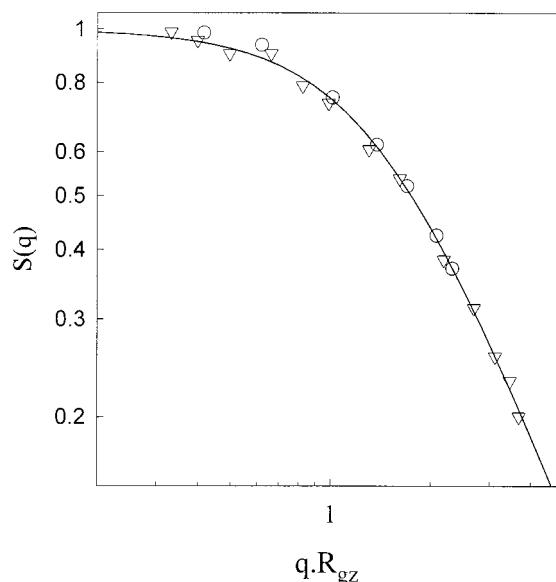


Figure 5. Static structure factor of branched PS based on precursors with $M_w = 1.0 \times 10^4$ g/mol (triangles) and 1.7×10^4 g/mol (circles). The solid line represents the static structure factor of branched PMMA.¹⁶

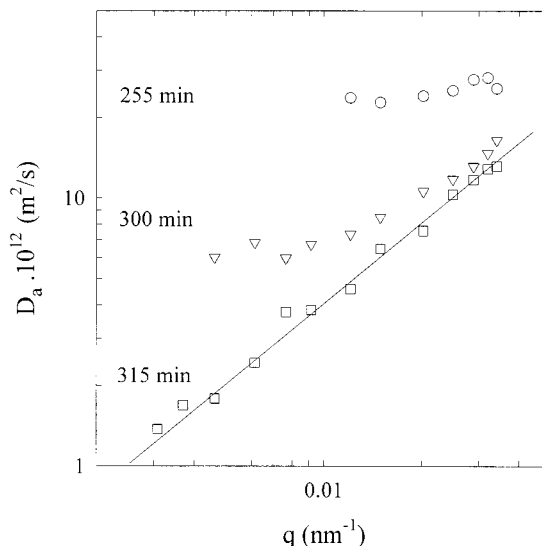


Figure 6. Double-logarithmic representation of the q dependence of D_a at different heating times indicated in the figure. The straight line has slope 1 .

PMMA have the same large-scale structure. Of course, the structure is different on length scales smaller than the radius of the precursors. However, these length scales cannot be accessed in the q range covered by light scattering.

The intensity autocorrelation correlation functions of the samples at different heating times were very similar to those of cross-linked PMMA reported earlier.¹⁶ The data could be accurately described by a monomodal distribution of relaxation times (see Experimental Section). In Figure 6 the apparent diffusion coefficient is plotted as a function of q for various heating times. At short times D_a is independent of q , but the q dependence increases with increasing reaction time. At $t_h = 315$ min we observe that $D_a \propto q$ over the whole accessible q range, and Figure 3 shows that we are probing the internal dynamics for this sample. The linear q dependence of D_a is expected for fully flexible polymers¹ if $qR_g \gg 1$. The data superimpose if D_a/D_0 is plotted as a

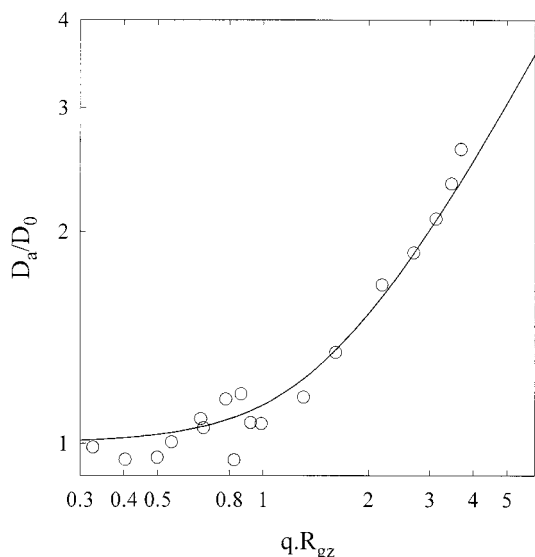


Figure 7. Comparison of the dependence of D_a/D_0 on qR_{gz} for branched PS (circles) and branched PMMA (solid line).¹⁶

function of qR_{gz} (see Figure 7), and the solid line through the data demonstrates that the behavior is the same as for cross-linked PMMA.¹⁶

For highly diluted samples we may neglect the effect of interactions and calculate the z -average hydrodynamic radius (R_{hz}) from D_a extrapolated to $q = 0$: $R_{hz} = kT/(6\pi\eta D_0)$,²³ with k_B Boltzmann's constant, T the absolute temperature, and η the solvent viscosity. R_{hz} could be obtained even for the smaller samples for which R_{gz} could not be determined accurately. For the larger samples we find that $R_{gz}/R_{hz} \approx 2$, which is shown in Figure 4 where values of $2R_{hz}$ are compared with R_{gz} . For cross-linked PMMA it was found that $R_{gz}/R_{hz} = 2.1$,¹⁶ while for cross-linked PDMS $R_{gz}/R_{hz} = 1.7$. Notice that the value of R_{gz}/R_{hz} is influenced by polydispersity because $R_{gz} = \langle R_g^2 \rangle_z^{0.5}$ and $R_{hz} = \langle R_h^{-1} \rangle_z^{-1}$, which means that $R_{gz}/R_{hz} > R_g/R_h$. The effect of polydispersity on R_{gz}/R_{hz} depends not just on τ and d_f , as was assumed by Adam et al.,¹⁷ but also on the cutoff function in eq 1. For particles with a self-similar structure we expect that both R_{gz} and R_{hz} have a power law dependence on M_w . From a linear least-squares fit of the data in Figure 4 we find $d_f^* = 1.6$, which is consistent with the value obtained from the structure factor of the very large branched polymers formed at $t = 315$ min.

The main result from this study is that the large-scale structure of branched PS is the same as that of branched PMMA within the experimental error, despite the very different local structure. In addition, although we did not compare the results with the full structure factor

of branched PDMS, the limiting power law q dependence at large qR_{gz} is the same. The agreement is a strong indication that the gel formation of flexible polymeric gels is a universal process. The formation of PMMA gels was studied and discussed elsewhere in much greater detail.^{15,16} The close correspondence of cross-linked PMMA with cross-linked PS studied here means that there is no need to discuss the present system in greater detail. For both systems the percolation model appears to describe the gel formation correctly, but as was discussed in the Introduction, it is very difficult to verify this model experimentally.

References and Notes

- (1) de Gennes, P. G. *Scaling Concepts in Polymer Physics*; Cornell University Press: Ithaca, NY, 1979.
- (2) Stauffer, D.; Aharony, A. *Percolation Theory*, 2nd ed.; Taylor & Francis: London, 1992.
- (3) Lorentz, C. D.; Ziff, R. D. *Phys. Rev. E* **1998**, *57*, 230.
- (4) Grassberger, P. *J. Phys. A: Math. Gen.* **1992**, 5867.
- (5) Gimel, J. C.; Durand, D.; Nicolai, T. *J. Sol-Gel Sci. Technol.* **1998**, *15*, 129.
- (6) Gordon, M. *Proc. R. Soc. London* **1962**, A268, 240.
- (7) Schosseler, F.; Benoit, H.; Gubisic-Gallot, Z.; Strazielle, Cl.; Leibler, L. *Macromolecules* **1989**, *22*, 400.
- (8) Patton, E. V.; Wesson, J. A.; Rubinstein, M.; Wilson, J. C.; Oppenheimer, L. E. *Macromolecules* **1989**, *22*, 1946.
- (9) Bauer, J.; Burchard, W. *Macromolecules* **1993**, *26*, 3103.
- (10) Degoulet, C.; Nicolai, T.; Durand, D.; Busnel, J. P. *Macromolecules* **1995**, *28*, 6819.
- (11) Gimel, J. C.; Nicolai, T.; Durand, D.; Teuler, J. M. *Eur. Phys. J. B* **1999**, *12*, 91.
- (12) Prochazka, F.; Nicolai, T.; Durand, D. *Macromolecules* **2000**, *33*, 1703.
- (13) See e.g.: Nicolai, T.; Durand, D.; Gimel, J. C. In *Light Scattering. Principles and Developments*; Brown, W., Ed.; Clarendon Press: Oxford, 1996.
- (14) Cates, M. E. *J. Phys., Lett.* **1985**, *46*, 757.
- (15) Lesturgeon, V.; Nicolai, T.; Durand, D. *Eur. Phys. J. B* **1999**, *12*, 71.
- (16) Lesturgeon, V.; Nicolai, T.; Durand, D. *Eur. Phys. J. B* **1999**, *12*, 83.
- (17) Adam, M.; Lairez, D.; Karpasas, M.; Gottlieb, M. *Macromolecules* **1997**, *30*, 5920.
- (18) Ourdouillie, P. Ph.D. Thesis, Lyon, 2000.
- (19) See e.g.: *Light Scattering from Polymer Solutions*; Huglin, Ed.; Academic Press: London, 1972. Higgins, J. S.; Benoit, K. C. *Polymers and Neutron Scattering*; Clarendon Press: Oxford, 1994. Brown, W., Ed.; *Light Scattering. Principles and Developments*; Clarendon Press: Oxford, 1996.
- (20) Finnigan, J. A.; Jacobs, D. J. *Chem. Phys. Lett.* **1970**, *6*, 141.
- (21) Moreels, E.; De Ceunick, W. *J. Chem. Phys.* **1987**, *86*, 618.
- (22) Pedley, A. M.; Higgins, J. S.; Peiffer, D. G.; Burchard, W. *Macromolecules* **1990**, *23*, 434.
- (23) Berne, B.; Pecora, R. *Dynamic Light Scattering*; Wiley: New York, 1976.
- (24) Nicolai, T.; Gimel, J. C.; Johnsen, R. *J. Phys. II* **1996**, *6*, 697.
- (25) Stepanek, P. In *Dynamic Light Scattering*; Brown, W., Ed.; Oxford University Press: New York, 1993.

MA010113I